Using Holo-Hilbert Spectral Analysis (HHSA) to analyze EEG Oscillatory during Repetitive Movements

Hao-Teng Hsu[1], Kuo-Kai Shyu[1], and Po-Lei Lee[1*]
[1]Department of Electrical Engineering, National Central University, Jhong Li, Taiwan.

***Abstract*—Neural oscillatory activities existing in multiple frequency bands usually represent different levels of neurophysiological meanings, from micro-scale to macro-scale organizations. In this study, we adopted Holo-Hilbert spectral analysis (HHSA) to study the amplitude-modulated (AM) and frequency-modulated (FM) components in sensorimotor Mu rhythm, induced by slow- and fast-rate repetitive movements. We observed that the instantaneous power induced by slow-rate movements was significantly higher than that induced by fast-rate movements ($p < 0.01$, Wilcoxon signed rank test). The alpha-band AM frequencies induced by slow-rate movements were higher than those induced by fast-rate movements, while no statistical difference was found in beta-band AM frequencies. The discrepancy between slow- and fast-rate movements might be owing to the change of motor functional modes from default mode network (DMN) to automatic timing with the increase of movement rates. The use of HHSA for oscillatory activity analysis can be an efficient tool to provide informative interaction among different frequency bands.**

***Index Terms*— Holo-Hilbert Spectral Analysis (HHSA), Motor Cortex, Repetitive movement**

I. Introduction

Motor control is crucial for people to interact with external environments. The production of body movements requires the integration of brain/cognition with sensory information to activate and coordinate the muscles, involved in the motion performance. To achieve a successful movement, several brain regions, including primary motor cortex, pre-motor cortex, supplementary motor area, frontal lobe, basal ganglia, cerebellum, etc., are involved and co-operated to generate desired movements. Execution of precise movement depends on the well control of skeletal muscles and the capability of internal time estimation [1]. Morillon et al. proposed the internal time estimation is a dual system which produces repetitive short durations in automatic mode (automatic timing) and requires more cog-nitive demand in default mode network (DMN) mode to track long durations [2]. Nevertheless, most of those literatures which studied the relation between time estimation and motor control are based on behavior data. Studying the brain activities induced by different movement rates will be helpful to shed light on unveiling the working mechanism of motor control.

Electroencephalography (EEG), which has the advantages of cheap, easy to preparation, and high temporal resolution, is widely used to study motor responses in human brain. However, several studies utilized linear approaches, such as event-related desynchronization/ synchronization (ERD/ERS), temporal spectral evolution (TSE), wavelet, and short-time Fourier transform (STFT), with pre-defined or stereotypical basis to interpret motor planning execution and post-movement inhabitation which leave non-stationary and non-linear parts in brain wave untreated [3]. In order to delineate both the non-stationary and non-linear features in a signal, Huang *et al.* has proposed a Holo-Hilbert spectral analysis (HHSA) method [4]. The HHSA is evolved from Hilbert-Huang transform (HHT) which is a full-informational spectral analysis method. The signal processing of HHSA contains a nested empirical mode decomposition (EMD) with the HHT which enables additive and multiplicative features can be resolved on a Holo-Hilbert spectrum (HHS). This research focused on studying the intra- and inter-scale spectral information during the execution of repetitive movements.

II. Materials and Methods

A. Subjects and Experiments

Ten right-handed healthy subjects (six males and four females, aged between 23 and 29 years old) with no history of neurological disease were recruited. Each subject was requested to participate in two repetitive-movement experiments with inter-movement intervals (IMI) of 7 s and 1 s, i.e., 0.14 Hz and 1 Hz, referring to slow- and fast-rate movements, respectively. EEG data were recorded by a sixteen-channel EEG system (Vamp Amp., Brain Products, Munich, Germany). Two EEG channels were used to cover motor-area regions (C3 and C4), with respect to a reference electrode placed at right mastoid and a ground electrode placed at left mastoid. The EEG data were sampled at 2 k Hz (band-pass, 0.05-100 Hz; band-stop, 60 Hz) with the impedance kept below 5 kΩ for all electrodes.

B. Holo-Hilbert Spectral Analysis (HHSA)

In this study, we assumed the EEG signal recorded from motor area contained a number of frequency components, in which each frequency component was modulated by its characteristic amplitude function. Therefore, a two-layer EMD architecture was adopted [5]. In the first layer, the EEG signal was decomposed into a series of IMFs, denoted as IMF_{FM}s, representing as a dyadic filter bank to accommodate the frequency features into distinct frequency-modulated (FM) modes. In the second-layer EMD, the upper envelopes of the IMF_{FM}s were further decomposed into a set of amplitude-modulated (AM) IMFs, denoted as IMF_{AM}s, to analyze the inter-mode interactions among IMF_{FM}s. The instantaneous frequencies

H. T. Hsu is with the Department of Electrical Engineering, National Central University, Taiwan (e-mail: fifaworld91@g.ncu.edu.tw).

K. K. Shyu is with the Department of Electrical Engineering, National Central University, Taiwan (e-mail: kkshyu@ee.ncu.edu.tw).

P. L. Lee* is with the Department of Electrical Engineering, National Central University, Taiwan (e-mail: pllee@ee.ncu.edu.tw) (corresponding author).

of IMF_{FM}s and IMF_{AM}s were then calculated using instantaneous frequency analysis technique to obtain the carrier-wave frequency FM (ω) and envelope-modulation frequency AM (Ω) frequencies. The ω and Ω frequencies were incorporated with its corresponding instantaneous power to construct a three-dimensional Holo-Hilbert spectrum (HHS) representation.

Fig. 1 shows a demonstration case of applying the HHSA to a simulated signal $X(t)$. The $X(t)$ was the addition of a frequency-modulated sinusoidal wave $X_1(t)$ with a white noise $N(t)$ (see Fig. 1(a)). The $X_1(t)$ was a 10 Hz sinusoidal wave modulated by a 2 Hz modulation wave, in which the 10 Hz wave was generated to simulate the alpha-band brain wave. Fig. 1(b) shows the IMF_{FM}s and IMF_{AM}s of the simulated signal decomposed by HHSA. Due to the limited space, only the first four IMF_{FM}s and their first four IMF_{AM}s were shown. The second IMF_{FM} (marked by green dashed rectangle) and its first IMF_{AM} (marked by red dashed rectangle), which had their mean frequencies of 10.06 Hz and 2.03 Hz, were recognized as the 10 Hz carrier wave and its 2 Hz modulation wave of $X_1(t)$, respectively. Calculating the instantaneous FM and AM frequencies of IMF_{FM}s and IMF_{AM}s, the HHS of $X(t)$ is shown in Fig. 1(c), in which the x-axis and y-axis represent the frequencies of ω and Ω, respectively, and the $P(\omega, \Omega)$ is scaled by taking 4-th root, i.e., $P(\omega, \Omega)^{0.25}$ [6], to facilitate data display. It can be observed that two clear contours centered at (ω, Ω) = (10.06 Hz, 2.03 Hz) and (ω, Ω) = (10.06 Hz, 0.05 Hz). The modulation frequencies Ω at 2.03 Hz and 0.05 Hz indicate the 2 Hz modulation wave and its DC component, respectively. Since the white noise $N(t)$ is a wide-band signal without modulation, the $N(t)$ on HHS is represented by the contour with wide distributed carrier frequencies ω, from 0 to 25 Hz, and low modulation frequency, $\Omega \approx 0$ Hz.

C. *Determination of significant AM and FM frequencies on HHS*

To facilitate the quantifications of activation power and frequencies of Mu rhythm on HHS, two region-of-interests (ROIs), one for alpha band (8 Hz ≤ ω ≤ 16 Hz) and the other for beta band (16 Hz ≤ ω ≤ 24 Hz) [7, 8] with the modulation frequency range of 0.1 Hz ≤ Ω ≤ 3 Hz, were defined. Since the acquired EEG signals are inevitably contaminated with unexpected noise, left-tailed z-test was adopted to exclude those non-significant values on HHS by removing $P(\omega, \Omega)$ with z-test values smaller than -1.645 ($p < 0.05$). The rest of $P(\omega, \Omega)$ were selected, denoted as $P_s(\omega, \Omega)$, and were chosen for the subsequent calculations of total power and mean frequencies in ROIs. The total power of $P_s(\omega, \Omega)$ is calculated as:

$$P_{total} = \iint P_s(\omega, \Omega) d\omega d\Omega \quad , (3)$$

where P_{total} is the total power of $P_s(\omega, \Omega)$. The mean FM and AM frequencies of $P_s(\omega, \Omega)$, denoted as ω_{cf} and Ω_{cf}, in alpha (or beta) ROI are calculated as:

$$\omega_{cf} = \frac{\int \omega [\int P_s(\omega,\Omega) d\Omega] d\omega}{\int [\int P_s(\omega,\Omega) d\Omega] d\omega}$$
$$\Omega_{cf} = \frac{\int \Omega [\int P_s(\omega,\Omega) d\omega] d\Omega}{\int [\int P_s(\omega,\Omega) d\omega] d\Omega} \quad , (4)$$

where ω_{cf} and Ω_{cf} are the mean frequencies of FM and AM frequencies, respectively.

III. Results

This study ignored the handedness effect. The EEG activations were analyzed separately in hemispheres contralateral and ipsilateral to movement hands. Fig. 2 shows the P_{total}, ω_{cf}, and Ω_{cf} values in alpha and beta ROIs from C3 channel in subject S3 when he was performing right-hand finger lifting movements with slow and fast rates. For slow-rate movement (see Fig. 2(a)), the values of total power P_{total} for alpha and beta ROIs are 1.51 μV^2 and 0.70 μV^2, respectively. The mean frequencies (ω_{cf}, Ω_{cf}) for alpha and beta ROIs are (9.06 Hz, 0.88 Hz) and (19.86 Hz, 0.27 Hz) in slow-rate movements, respectively. For fast-rate movements (see Fig. 2(b)), the values of total power P_{total} for

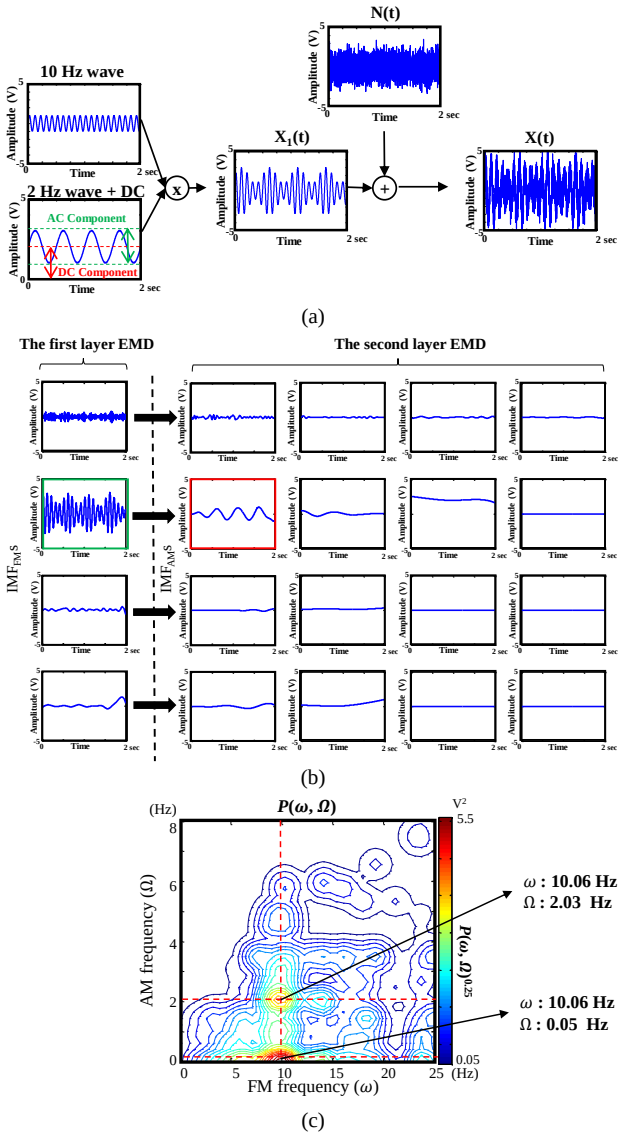

Fig. 1 (a) The $X_1(t)$ is the 10 Hz sinusoidal wave multiplied by a 2 Hz modulation. The $N(t)$ is a white noise, and the $X(t)$ is the addition of the $X_1(t)$ with $N(t)$. (b) The IMF_{FM}s of the $X(t)$ are decomposed by the first-layer EMD. The pattern of multiplicative modulation can be seen in the second IMF_{FM} (marked by green dashed rectangle). The upper envelope of each IMF_{FM} are then decomposed into its IMF_{AM}s by the second- layer EMD. The pattern of modulation can be observed in the first IMF_{AM}, decomposed from the second IMF_{FM} (marked by red dashed rectangle). (c) The HHS for the $X(t)$ reveals two clear contours, one is at (ω, Ω) = (10.06 Hz, 2.03 Hz), and the other is at (ω, Ω) = (10.06 Hz, 0.05 Hz).

alpha and beta ROIs are 0.55 μV^2 and 0.11μV^2, respectively. The mean frequencies (ω_{cf}, Ω_{cf}) for alpha and beta ROIs are (9.74 Hz, 0.23 Hz) and (19.87 Hz, 0.35 Hz) in fast-rate movements, respectively.

Fig. 3 presents the P_{total} induced by slow-rate and fast-rate movements in the contralateral and ipsilateral sensorimotor cortexes. In Fig. 3(a), the P_{total} of alpha ROIs for slow-rate and fast-rate movements are 1.30 ± 0.48 μV^2 and 0.61 ± 0.33 μV^2 on contralateral hemispheres, and are 1.54 ± 0.65 μV^2 and 0.61 ± 0.37 μV^2 on ipsilateral hemispheres, respectively. In Fig. 3(b), the P_{total} of beta ROIs for slow-rate and fast-rate movements are 0.70 ± 0.48 μV^2 and 0.29 ± 0.20 μV^2 on contralateral hemispheres, and are 0.69 ± 0.39 μV^2 and 0.28 ± 0.18 μV^2 on ipsilateral hemispheres, respectively. In both the contralateral and ipsilateral hemispheres, the

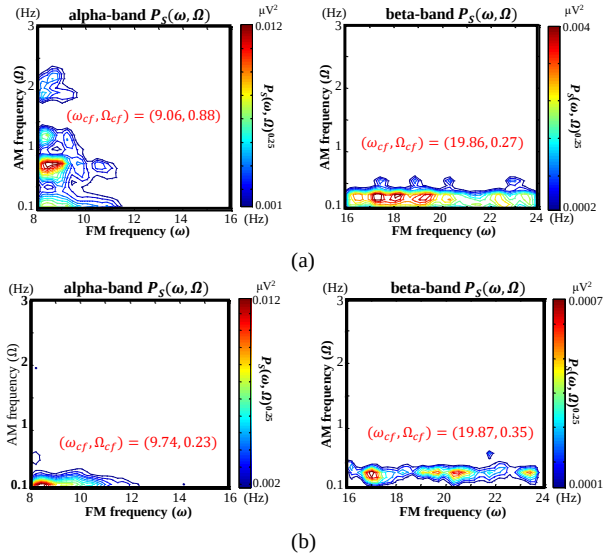

Fig. 2 The HHS on C3 channel in right-hand repetitive movements. (a) In slow-rate repetitive movements, the P_{total}, ω_{cf}, and Ω_{cf} of the alpha-band $P_S(\omega, \Omega)$ are 1.51 μV^2, 9.06 Hz, 0.88 Hz, and are 0.70 μV^2, 19.86 Hz, 0.27 Hz for beta-band $P_S(\omega, \Omega)$, respectively. (b) In fast-rate repetitive movements, the P_{total}, ω_{cf}, and Ω_{cf} of the alpha-band $P_S(\omega, \Omega)$ are 0.55 μV^2, 9.74 Hz, 0.23 Hz, and are 0.11 μV^2, 19.87 Hz, 0.35 Hz for beta-band $P_S(\omega, \Omega)$, respectively.

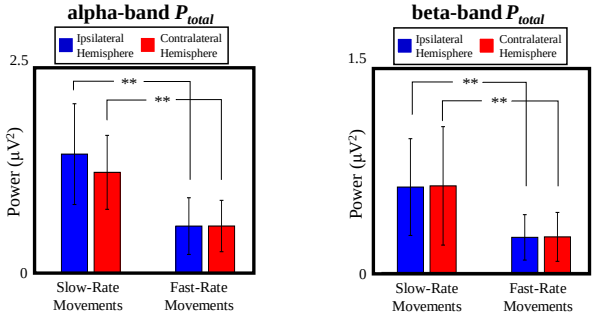

Fig. 3 Comparison of the averaged P_{total} over all subjects in (a) alpha band and (b) beta band. ** indicates significant difference between conditions at $p < 0.01$.

values of slow-rate movements induced P_{total} were higher than those induced by fast-rate movements in both the alpha and beta bands ($p < 0.01$, Wilcoxon signed rank test). Comparing the P_{total} of contralateral hemisphere with ipsilateral hemisphere, no significant difference was found in slow-rate movements ($p = 0.56$ for alpha-band, $p = 0.68$ for beta band; Wilcoxon signed rank test) and in fast-rate movements ($p = 0.88$ for alpha-band, $p = 0.53$ for beta band; Wilcoxon signed rank test).

Fig. 4 shows the ω_{cf} and Ω_{cf} for slow-rate and fast-rate movements in alpha and beta bands. In Fig. 6(a), the alpha-band ω_{cf} for slow-rate and fast-rate movements are 10.35 $\pm$ 1.23 Hz and 10.59 $\pm$ 1.29 Hz in contralateral hemispheres, and are 10.39 $\pm$ 1.21 Hz and 10.54 $\pm$ 1.28 Hz in ipsilateral hemispheres, respectively. The modulation frequencies Ω_{cf} of alpha-band ω_{cf} for slow-rate and fast-rate movements are 0.75 $\pm$ 0.17 Hz and 0.53 $\pm$ 0.21 Hz in contralateral hemispheres, and are 0.63 $\pm$ 0.22 Hz and 0.66 $\pm$ 0.35 Hz in ipsilateral hemispheres, respectively. It can be observed that the modulation frequencies Ω_{cf} in contralateral hemispheres induced by fast-rate movements are significantly lower than those induced by slow-rate movements ($p < 0.01$; Wilcoxon signed rank test), while no significant

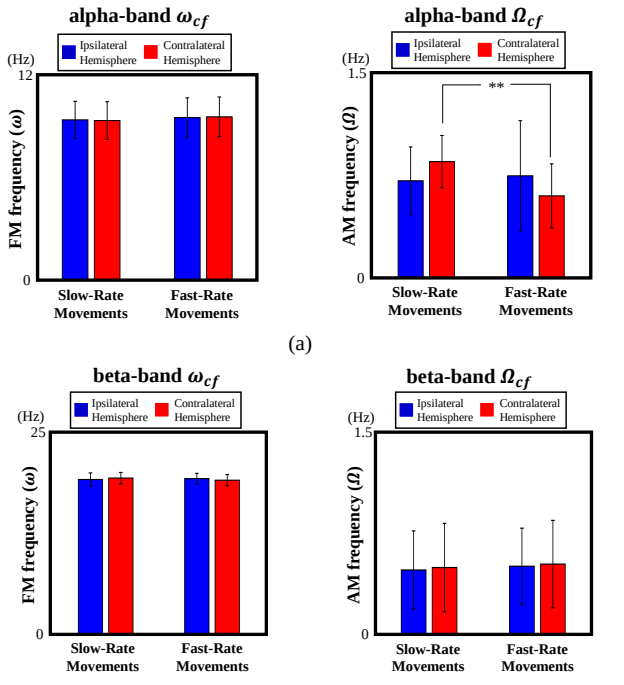

Fig. 4 Comparison of the averaged ω_{cf} and Ω_{cf} over all subjects in (a) alpha band and (b) beta band. ** indicates significant difference between conditions at $p < 0.01$.

difference in alpha-band Ω_{cf} was found in ipsilateral hemispheres ($p = 0.63$; Wilcoxon signed rank test). Besides, no significant difference in alpha-band ω_{cf} was found between slow-rate and fast-rate movements in both contralateral hemispheres ($p = 0.12$; Wilcoxon signed rank test) and ipsilateral hemispheres ($p = 0.47$; Wilcoxon signed rank test).

In beta band (Fig. 4(b)), the beta-band ω_{cf} for slow-rate and fast-rate movements are 19.33 $\pm$ 0.69 Hz and 19.07 $\pm$ 0.70 Hz in contralateral hemispheres, and are 19.16 $\pm$ 0.82 Hz and 19.26 $\pm$ 0.65 Hz in ipsilateral hemispheres, respectively. The modulation frequencies Ω_{cf} of beta-band ω_{cf} for slow-rate and fast-rate movements are 0.46 $\pm$ 0.31 Hz and 0.48 $\pm$ 0.30 Hz in contralateral hemispheres, and are 0.44 $\pm$ 0.27 Hz and 0.47 $\pm$ 0.26 Hz in ipsilateral hemispheres, respectively. No significant difference was found for both the ω_{cf} and Ω_{cf} in contralateral and ipsilateral hemispheres while performing slow-rate and fast-rate movements ($p > 0.41$; Wilcoxon signed rank test).

IV. Discussion

This study took the advantage of HHSA in full spectral representation and applied it to investigate brain oscillatory activities induced by different movement rates. The HHSA provides not only the FM components but also the AM components of the measured signals. It describes the FM-AM representation across different carrier frequencies and efficiently analyzes the cross-frequency phase-amplitude interaction, which is also known as phase-amplitude coupling (PAC) [9]. The HHSA is a systematic analysis approach by means of applying nested EMD and HHT to interpret the PAC phenomenon in brain waves. Compared to other PAC approaches which have to filter the measured signals into predefined frequency bands for phase-coupling analyses, the HHSA decomposes the input signal into IMF_{FM}s by applying first-layer EMD and then applies second-layer EMD to extract IMF_{AM}s for the interpretation of cross-scale phase-amplitude interactions. In our study, the HHSA effectively investigate the modulation changes of Mu rhythms induced by slow- and fast-rate movements. Since the oscillatory activities of distinct

frequency bands represent different levels of neurophysiological meanings from micro-scale to macro-scale organizations, it is worthy to study the PAC across different frequency ranges which might provide a window to explain the intricate working mechanism of underlying neuronal substrates.

Current PAC techniques usually confine the measured signals into stereotypical sub-bands by applying linear filtering techniques, and then calculate PAC factors using cross-frequency coupling techniques, such as mutual information (MI) [10], coherence [11], phase-locking factor (PLF) [12], etc. Nevertheless, owing to the nonstationary nature of brain waves, the utilization of pre-defined filter bank might cause the pitfall of not being able to well extract meaningful signal features for PAC calculation. In contrast, the HHSA is established based on data-driven approach using EMD. The EMD decomposes a signal into a collection of analytic intrinsic mode functions (IMF), representing coarse-to-fine information, which enables the local features of a signal to be characterized by iteratively applying a sifting process. Each IMF is an analytic, self-constructed, well-defined function with time-varying amplitudes and frequencies. The full-informational spectral display of HHS provides an intuitive view to represent the interaction of envelope modulations among multi-scale carrier waves.

With the advantage of full-informational spectral analysis of HHSA, the HHSs obtained from slow-rate and fast-rate repetitive movements can be measured and compared. In Fig. 4, the fast-rate movements show a consistent AM modulation frequency Ω_{cf} around 0.25 Hz across alpha and beta bands, while discrepancy between alpha- and beta-band Ω_{cf} were observed in the performing of slow-rate movements. In addition, the mean frequencies of alpha-band Ω_{cf} in slow-rate movements are significant higher than those in fast-rate movements, while no statistical difference was observed in beta-band Ω_{cf} between slow-rate movements and fast-rate movements. According to Basar *et al.* [13], since the signals of lower- and higher-frequency oscillatory activities could act as communication signals for large-scale and local-scale resonant systems, respectively [14]. The consistency of Ω_{cf} across alpha and beta band in fast-rate movements could indicate the strong coupling between alpha and beta bands (see Fig. 4), representing the information transferring between large-scale brain networks and local cortical processing. The observation might echo Toma's study, which utilized coherent technique to probe cortical coupling during different movement rates and found motor cortices were continuously coupled in faster repetitive movements [15].

V. CONCLUSION

This paper proposes a HHSA-based approach to systematically analyze the FM and AM components from the sensorimotor Mu rhythms induced by repetitive movements. The adopted HHSA is a two-layer EMD architecture, which firstly decomposes the EEG signal into a series of IMF_{FM}s and then decomposes each IMF_{FM} into a set of IMF_{AM}s. The salient features of the HHSA–based approach are as follows: 1) the HHSA utilizes EMD to extract FM and AM information which enables the time-varying amplitude and frequency features to be retained in IMFs; 2) the instantaneous frequencies (ω, Ω) of IMF_{FM}s and IMF_{AM}s are incorporated with their instantaneous power $P(\omega, \Omega)$ to achieve HHS for full-informational spectral analysis; 3) the HHS statistically represents the power density of the measured signal on the FM-AM axes which allows (ω, Ω) with insignificant power density can be identified; 4) the P_{total}, ω_{cf} and Ω_{cf} obtained from slow-rate and fast-rate movements are calculated and compared; Our study demonstrates the efficacy of HHSA in analyzing brain oscillatory activities which provides an insightful view on subtle brain dynamics.

VI. REFERENCE

1. Gavazzi, G., A. Bisio, and T.J.S.r. Pozzo, *Time perception of visual motion is tuned by the motor representation of human actions.* 2013. **3**(1): p. 1-8.
2. Morillon, B., C.A. Kell, and A.-L.J.J.o.N. Giraud, *Three stages and four neural systems in time estimation.* 2009. **29**(47): p. 14803-14811.
3. Thut, G., C. Miniussi, and J. Gross, *The functional importance of rhythmic activity in the brain.* Current Biology, 2012. **22**(16): p. R658-R663.
4. Huang, N.E., et al., *On Holo-Hilbert spectral analysis: a full informational spectral representation for nonlinear and non-stationary data.* Phil. Trans. R. Soc. A, 2016. **374**(2065): p. 20150206.
5. Huang, N., *The Empirical Mode Decomposition Method and The Hilbert Spectrum For Non-Stationary Time Series.* Proc. Roy. Soc. London, 45AA, 1998: p. 703-775.
6. Huang, N.E., et al., *On Holo-Hilbert spectral analysis: a full informational spectral representation for nonlinear and non-stationary data.* 2016. **374**(2065): p. 20150206.
7. Shindo, K., et al., *Effects of neurofeedback training with an electroencephalogram-based brain–computer interface for hand paralysis in patients with chronic stroke: a preliminary case series study.* Journal of rehabilitation medicine, 2011. **43**(10): p. 951-957.
8. Lee, S. and S.-Y. Lee. *ICA-Based Spatio-temporal Features for EEG Signals*. in *International Conference on Neural Information Processing*. 2007. Springer.
9. Samiee, S., et al., *Phase-amplitude coupling.*
10. Tort, A.B., et al., *Measuring phase-amplitude coupling between neuronal oscillations of different frequencies.* Journal of neurophysiology, 2010. **104**(2): p. 1195-1210.
11. Onslow, A.C., R. Bogacz, and M.W. Jones, *Quantifying phase–amplitude coupling in neuronal network oscillations.* Progress in biophysics and molecular biology, 2011. **105**(1): p. 49-57.
12. van der Meij, R., M. Kahana, and E. Maris, *Phase–amplitude coupling in human electrocorticography is spatially distributed and phase diverse.* Journal of Neuroscience, 2012. **32**(1): p. 111-123.
13. Başar, E., et al., *Brain oscillations in perception and memory.* International journal of psychophysiology, 2000. **35**(2): p. 95-124.
14. Von Stein, A. and J. Sarnthein, *Different frequencies for different scales of cortical integration: from local gamma to long range alpha/theta synchronization.* International journal of psychophysiology, 2000. **38**(3): p. 301-313.
15. Toma, K., et al., *Movement rate effect on activation and functional coupling of motor cortical areas.* Journal of neurophysiology, 2002. **88**(6): p. 3377-3385.